TWENTY YEARS OF EXPERIENCE WITH A MODULAR DESIGN SYSTEM FOR CENTRIFUGAL PROCESS COMPRESSORS

by

Klaus Lüdtke

Manager Engineering/Development

Babcock-Borsig Aktiengesellschaft

Berlin, Germany

Klaus Lüdtke is Department Manager for Aerodynamic Design, Engineering and Development of Turbomachinery with Babcock-Borsig. He received the "Diplom-Ingenieur" degree in Mechanical Engineering from the Technical University of Berlin (1962). For the past 30 years, he has worked in the field of industrial centrifugal compressor design. Prior to joining Babcock-Borsig, he worked with Allis-Chalmers, Milwaukee (1969 to 1971), where he got the opportunity to develop the theory of the modular design system for centrifugal compressors described in this paper. Presently, he is in charge of aerothermodynamic and mechanical design, performance testing, component development, and support of project and sales activities through worldwide presentations of the company's compressor technology.

ABSTRACT

The design of single shaft horizontally split and barrel type compressors is based on a modular design system, which comprises fixed geometry components, i.e., impellers, diffusers, return vane channels, scrolls, and inlet ducts. The philosophy of the system is based on limited deviations from aerodynamic similarity.

The performance curves of each individual fixed geometry stage were deduced from aerodynamic measurements carried out either with atmospheric air (for the low convergency line) or with freon (for the high convergency line). The aerodynamic similarity principle assures the validity of these stage measurements for the operation with all other industrial gases, whose molecular weights range from 4.0 to 120.

INTRODUCTION

During numerous "technical clarification meetings" with engineering companies and end users, the author had to explain his company's centrifugal compressor design philosophy. Although it is a manufacturer's discretion how to design compressors, the very core of the technology raises great external interest, especially when it becomes known that one possible method is the modular concept, which uses just one fixed geometry impeller family to compress all relevant industrial gases. Since oral arguments in most cases were not sufficient to explain why the geometry is not changed when another gas is compressed, short descriptions were occasionally issued.

The following presentation, however, is intended to be a more fundamental and comprehensive report on the background and practical application of the modular system. It is hoped that it provides users with the information needed to understand the design approach.

Centrifugal process compressors of the single-shaft type are characterized by an almost infinite number of variation options. They compress gases with molecular weights between 4.0 and 120.0, covering volume flows within the region of 500 to 300,000 m^3/h and discharge pressures from below atmosphere to 800 bar, many with sidestreams or extractions. One to 20 impellers are arranged inline or back to back in up to three casings. They are either uncooled or have a maximum of three intercoolers per casing, resulting in a maximum number of eight nozzles on the casing. Process compressors are driven by electric motors, steam or gas turbines directly, or via a gear box between drive and compressor or between casings.

Such a vast array of combination options prohibits any package unit standardization as it is the case, e.g., for plant air or water chilling compressors, where the gas never changes and the pressure ratios are within narrow limits. Therefore, any attempt to bring about a standardization has to concentrate on the stage as the smallest element common to all process compressor variations.

The described modular design system is defined as a fixed relative geometry shrouded impeller family whose members represent discrete flow coefficients between 0.01 and 0.15 (Figure 1).

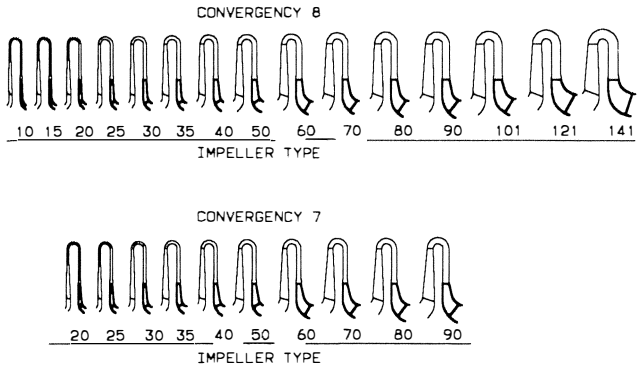

Figure 1. Modular Impeller Family.

Matching vaneless diffusers and return vane channels are assigned to each standard impeller, making up the complete modular stage. Impellers can also be combined with plenum inlets, when located downstream of a suction nozzle (Figure 2), or with volutes, when located upstream of a discharge nozzle (Figure 3). Standard sidestream arrangements are also available (Figure 4).

The inlet flow coefficient, however, is not sufficient to define the impeller geometry. The second parameter is the impeller volume ratio, which is a strong function of the molecular weight of the gas. This, in turn, influences the "convergency," i.e., the meridional area reduction from impeller inlet to exit. Each impeller at the given flow coefficient splits up into two convergencies, representing two discrete volume ratios, covering approximate

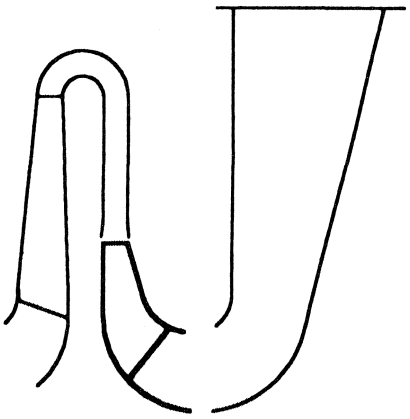

Figure 2. Module: Plenum Inlet/Impeller/Diaphragm.

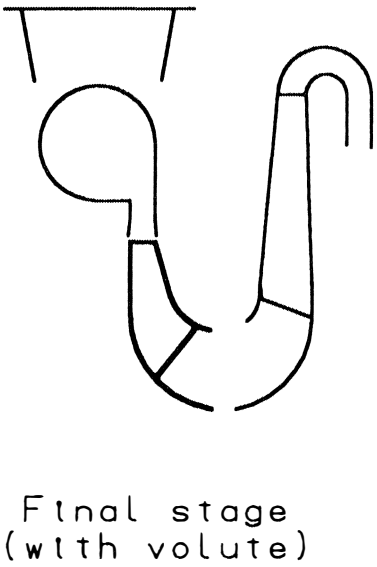

Figure 3. Module: Return Vane Inlet/Impeller/Volute.

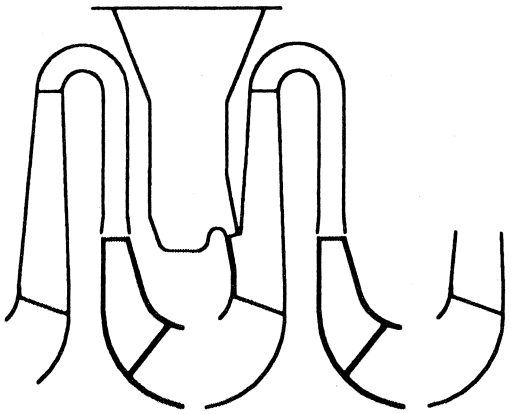

Figure 4. Module: Impeller/Sidestream/Impeller.

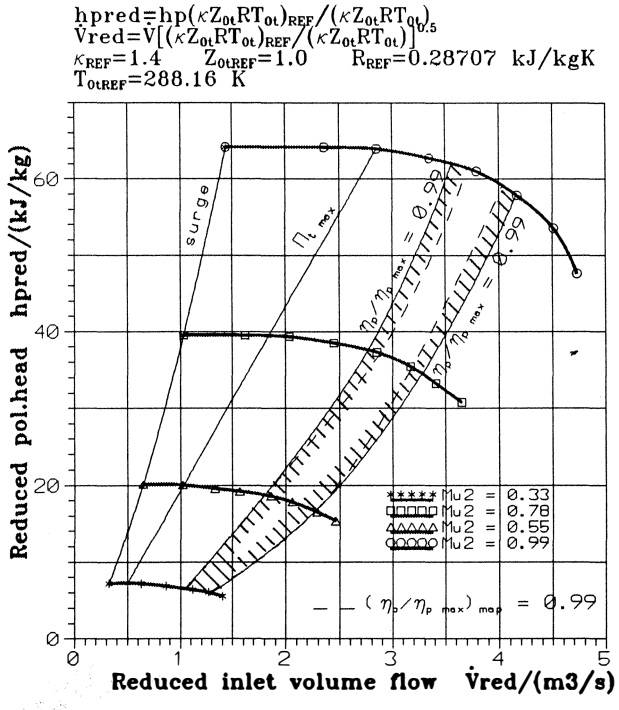

Figure 5. Measured Polytropic Head Curves.

molecular weights between 4.0 and 40.0 (upper line) and 35.0 to 120.0 (lower line).

So the complete family consists of 25 impeller types. Each of these impellers has a fixed geometry and is scaled within a range of between 200 and 1400 mm outer wheel diameter.

PHILOSOPHY

The key to understanding the fundamental principle of the modular system is "limited deviations from aerodynamic similarity."

Dimensional Performance Curves

The starting point is the variable speed map. Test values of a stage with a 400 mm impeller with 3-D blades arranged between a plenum inlet and a return-vane passage are shown as examples in Figures 5 and 6.

The following facts can be deduced from Figures 5 and 6:

- The stage efficiency changes very little within the very wide Mach number range of 0.33 to 0.99 and also within a certain flow range on each individual curve. The zone between the two dashed lines is the range where the stage efficiency does not drop off by more than one percent from the map efficiency maximum.

- The shaded area represents one percent efficiency drop-off from individual curve efficiency maxima. This volume flow zone, referred to as "rating range," is on a percentage basis relatively narrow at high Mach numbers (92 to 107 percent at $Mu_2 = 0.99$) and relatively wide at low Mach numbers (89 to 111 percent at $Mu_2 = 0.33$). One hundred percent flow refers to the curve's best efficiency point.

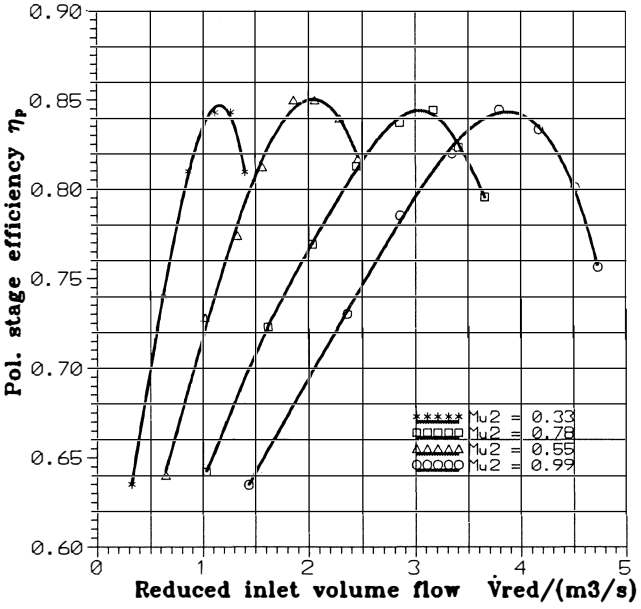

Figure 6. Measured Polytropic Efficiency Curves.

- The overall curve extension from surge to choke volume flow shrinks with increasing Mach number: 28 to 167 percent at Mu_2 = 0.33 and 37 to 126 percent at Mu_2 = 0.99.
- The volume flow, where the maximum pressure ratio is attained is 73 percent at Mu_2 = 0.99, 60 percent at Mu_2 = 0.78, 50 percent at Mu_2 = 0.55, and 43 percent at Mu_2 = 0.33.
- The polytropic head rise from optimum to surge reduces for increasing Mach numbers: 14 percent at Mu_2 = 0.33 and six percent at Mu_2 = 0.99.

All these observations are summarized for two Mach numbers in Figure 7.

Another fact can be deduced:
The inlet flow coefficient at the efficiency maximum of each curve drops when the Mach number is reduced: φ is 0.092 at Mu_2 = 0.99 and 0.083 at Mu_2 = 0.33.

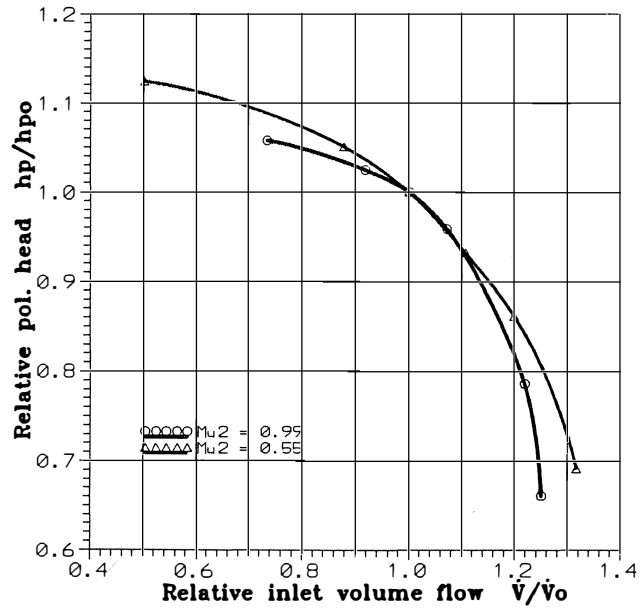

Figure 7. Mach Number Influence on Curve Shape.

The conclusions from all these facts, which can be found from any single-stage test with speed variation, are:

- The fixed geometry stage, designed for one defined operating point, can be used without any significant consequences for off-design operating points lying anywhere in the minus one percent range (shaded zone on Figure 5).

Neither operating range nor polytropic head rise have to be sacrificed. The maximum efficiency degradation is much lower than effects of manufacturing and metering tolerances. It has to be kept in mind that the optimum inlet flow coefficient (i.e., where the best efficiency point occurs) drops with falling Mach number.

Nondimensional Performance Curves

When a given compressor stage is operated under different conditions and with different gases, the laws of aerodynamic similarity must be satisfied.

The following similarity parameters play the decisive role in converting the dimensional performance map, Figures 5 and 6, into nondimensional performance curves that enable a performance prediction of the same stage with a different gas. There are four primary or independent similar parameters:

- To maintain similarity for the impeller inlet, the nondimensional inlet flow coefficient must be kept constant:

$$\varphi = \frac{\dot{V}_{0t}}{\frac{\pi}{4} d_2^2 u_2} \tag{1}$$

d_2 = impeller outer diameter

u_2 = impeller tip speed

Subscripts denote flow path location (Figure 19)

$\dot{V}_{0t}$ = volume flow including any recirculation flow from the balance piston referenced to the suction stagnation state.

The true static impeller inlet volume flow directly upstream of the blade leading edge is greater by the inlet expansion, due to the acceleration of the gas and by the shroud labyrinth leakage:

$$\varphi^* = \frac{\dot{V}_{0t} \frac{v_0}{v_{0t}} \frac{\Delta\dot{m}}{\dot{m}}}{\frac{\pi}{4} d_2^2 u_2} \tag{2}$$

v_0 = static specific volume upstream impeller leading edge

v_{0t} = total specific volume impeller suction side

$\Delta\dot{m}$ = shroud labyrinth leakage mass flow

$\dot{m}$ = process mass flow incl. balance piston leakage

A constant inlet flow coefficient assures the same blade incidence at the leading edge.

- To maintain similarity at the impeller exit and the diffuser inlet, the impeller exit flow coefficient must be kept constant:

$$\varphi_3 = \varphi \frac{\dot{V}_3/\dot{V}_{0t}}{4\, b_2/d_2} \tag{3}$$

$\dot{V}_3$ = static volume flow at impeller exit

b_2 = impeller exit width

Impeller total-to-static volume ratio for perfect gas behavior (see APPENDIX):

$$\frac{\dot{V}_3}{\dot{V}_{0t}} = \frac{1}{[1 + s^* (\kappa-1)\, r\, Mu_2^2]^x} \; ; \quad x = \frac{r+\kappa(\eta_{pL}-1)}{r(\kappa-1)} \tag{4}$$

κ = perfect gas isentropic exponent

η_{pL} = pol. impeller efficiency, total to total

Reaction:

$$r = 1 - \frac{\varphi_3^2+s^{*2}}{2s^*} \tag{5}$$

Slip factor:

$$s^* = \frac{c_{u3}}{u_2} \tag{6}$$

C_{u3} = circumferential velocity component at impeller exit

A constant impeller exit flow coefficient warrants flow similarity at the impeller exit and the diffuser inlet.

• To satisfy aerodynamic similarity, the compressibility of the flow between two locations in the flow passage must be preserved, which is taken care of by a constant Mach number. The widely known machine or tip speed Mach number is used here:

$$Mu_2 = \frac{u_2}{a_0} \tag{7}$$

with the sonic velocity defined at inlet total state.

For perfect gas behavior the Mach number is:

$$Mu_2 = \frac{u_2}{\sqrt{\kappa R T_{0t}}} \tag{8}$$

R = gas constant

T_{0t} = abs. temperature impeller inlet, total state

κ = ratio of heat capacities

• To preserve friction effects between the gas and the flow passage walls, the Reynolds number must be kept constant.

The machine Reynolds number is defined as:

$$Re = \frac{u_2 b_2}{\nu} \tag{9}$$

ν = kinematic viscosity

When, for a given stage, all of these four primary similarity parameters are kept constant, the other three secondary or dependent similarity parameters are guaranteed (all defined on a total to total basis).

• Work input factor:

$$s = \frac{\Delta h}{u_2^2} \tag{10}$$

Δh = Enthalpy rise, total to total

• Polytropic stage efficiency

$$\eta_p = \frac{h_p}{\Delta h} \tag{11}$$

h_p = pol. head total to total

• Polytropic impeller efficiency

$$\eta_{pL} = \frac{h_{pL}}{\Delta h} \tag{12}$$

h_{pL} = impeller pol. head, total to total

The widely used polytropic head coefficient:

$$\psi_p = \frac{h_p}{u_2^2/2} = 2s\eta_p \tag{13}$$

is a product of work input factor and polytropic stage efficiency and not a new parameter!

When these partially interdependent seven parameters (derivation of formulas—see APPENDIX) are maintained, aerodynamic similarity is preserved, regardless of operating conditions such as suction pressure, temperature, and rotational speed.

Therefore, it is appropriate to transform the measured variable speed stage performance map (Figures 5 and 6) into nondimensional performance curves, applying the described similarity characteristics (Figures 8, 9, 10, 11, and 12).

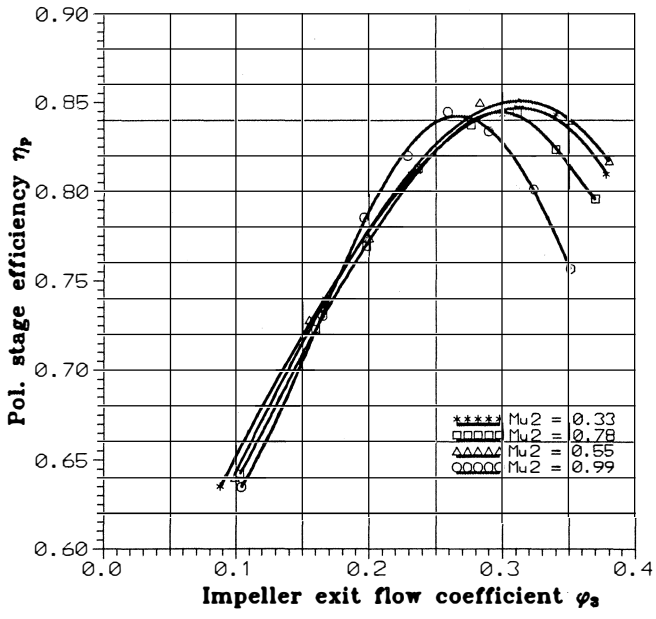

Figure 8. Nondimensional Curves, Pol. Efficiency.

For the first time, Sheets [1] showed that nondimensional curves become very simple for a wide range of Mach numbers when plotted as function of the impeller exit flow coefficient (which has by far a greater significance than the inlet flow coefficient),

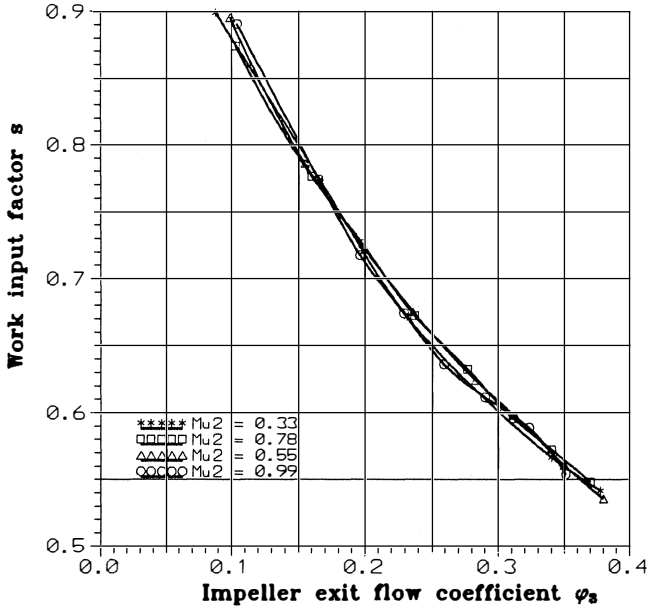

Figure 9. Nondimensional Curves, Work Input Coefficient.

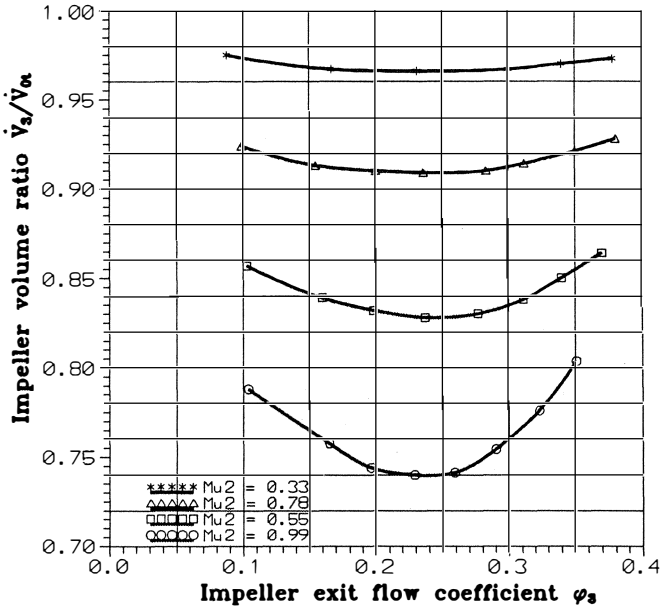

Figure 11. Nondimensional Curves, Impeller Volume Ratio.

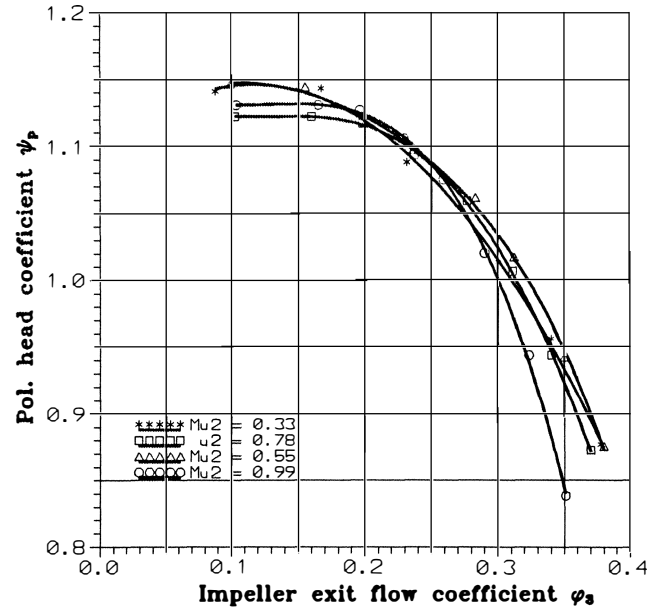

Figure 10. Nondimensional Curves, Pol. Head Coefficient.

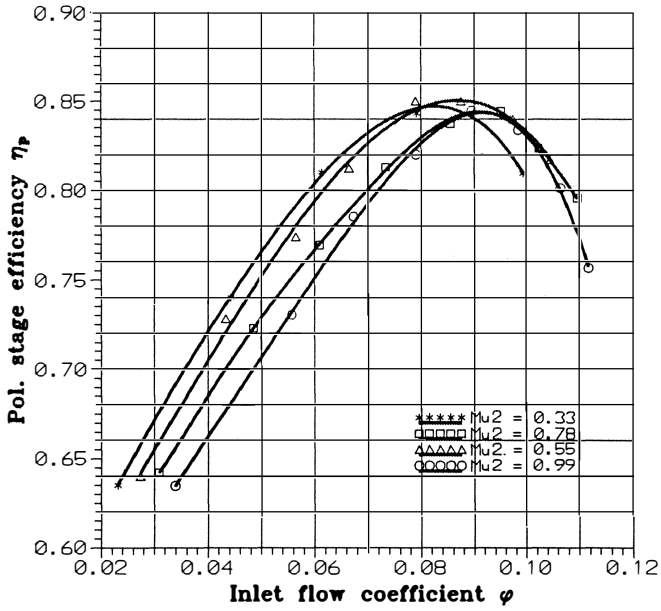

Figure 12. Nondimensional Curves, Efficiency vs *Inlet Flow Coefficient.*

because it directly connects work input to volume flow. This form of curves is used throughout the application of the modular design system. It shows work input factor and impeller and stage efficiency *vs* the impeller exit flow coefficient, with the tip speed Mach number as parameter. The charts do not explicitly show the inlet flow coefficient which, however, is implicitly included via Equations (3) through (6). The curves are valid for constant (test) Reynolds number. If it varies, efficiencies, work input factors, and flow coefficients have to be corrected as described by Strub, et al. [2].

The inlet flow coefficient (φ) is directly calculated from test values; outlet flow coefficient (φ_3) is iteratively calculated, using the measured work input factor s and corrected with the disk friction and shroud labyrinth leakage effect to arrive at the impeller slip s^* (see APPENDIX). The difference between s and s^* is significant only for very low flow coefficient impellers. The required impeller efficiency is calculated either from measured static pressure and calculated static temperature at the impeller exit, using energy and continuity equations (formula derived by Lüdtke [3]), or on the basis of a loss model, in case the static pressure is not available or not reliable. Even a reasonably estimated course of the impeller efficiency *vs* the exit flow coefficient is usable under the assumption that this estimate is consistently applied for test evaluation and future design purposes as well.

When plotting polytropic head coefficient, efficiency, and work input factor *vs* the exit flow coefficient, the following facts can be deduced from the test data (Figures 8 through 12):

- For Mach numbers up to approximately 0.6, the maximum efficiency occurs at a constant value of φ_3 (Figure 8).
- At higher Mach numbers the maximum efficiency is gradually shifted to lower values of φ_3 (Figure 8).
- The maximum efficiency changes within a narrow band of only ± 0.3 percent (which is smaller than the measuring tolerance); therefore, it is practically constant for Mach numbers between 0.33 and 0.99 (Figure 6).
- For all test Mach numbers, the work input coefficient becomes practically one single curve when plotted *vs* the impeller exit flow coefficient (Figure 9).
- The polytropic head coefficient for test Mach numbers 0.78 and lower lies in a narrow band of maximum ± one percent deviation. Accounting for the measuring tolerance, it is practically a single line versus φ_3. At $Mu_2 = 0.99$ the maximum flow coefficient φ_3 is reduced (Figure 10).
- All this happens although the impeller volume ratio $\dot{V}_3/\dot{V}_{ot}$ at the optimum φ_3 shows substantial variations between 0.74 and 0.97. This expresses a severe aerodynamic mismatching between the impeller exit and the inlet; i.e., considerable incidence angles at the blade leading edge without affecting the stage efficiency over wide Mach number changes (Figure 11).
- Consequently, if the stage efficiency is presented as function of the inlet flow coefficient φ (Figure 12), then the maximum efficiency occurs at different values of φ depending on the Mach number.

Rating Range

With this information, the rating range of this given measured stage can be established (Figure 13). It shows the impeller volume ratio *vs* inlet flow coefficient, including lines of constant impeller exit flow coefficient, lines of constant stage efficiency, referenced to the maximum, and lines of constant Mach numbers. The rating range limits are defined by an efficiency drop off of one percentage point, leading to the shaded rating range shape (Figure 13), which corresponds exactly with the shaded zone on Figure 5.

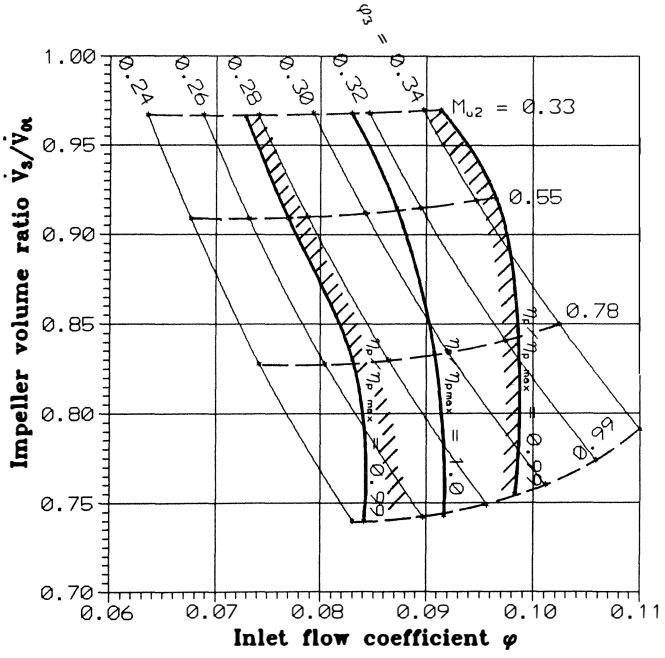

Figure 13. Stage Rating Range.

At low Mach numbers, constant efficiency lines follow the course of φ_3-lines; at high Mach numbers, efficiency lines are parallel to φ-lines.

The functional correlation between impeller volume ratio and Mach number is given by Equation (4) and shown in Figure 14 for two different isentropic exponents.

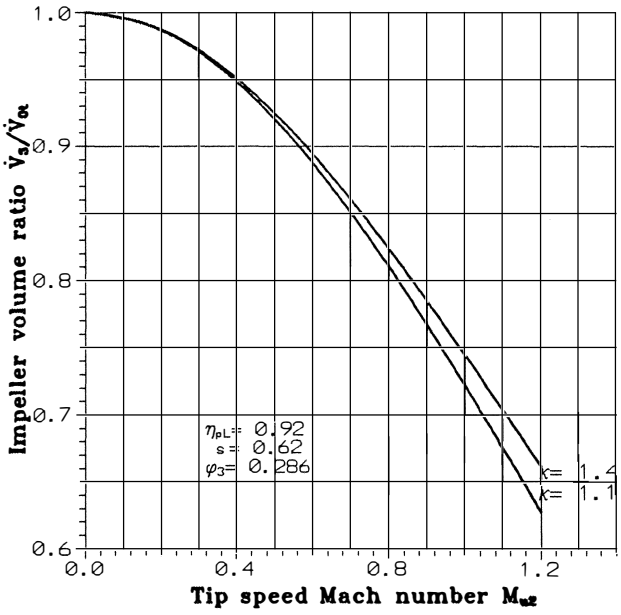

Figure 14. Impeller Volume Ratio vs *Mach Number.*

For impeller inlet/exit, matching the impeller volume ratio is, first of all, essential. To achieve the same volume ratio with a gas having a lower isentropic exponent, the Mach number has to be reduced, as can easily be seen from Figure 14.

Philosophy Summarized

The philosophy of the modular design system can be summarized as follows:

The impeller exit volume flow, nondimensionalized into the exit flow coefficient φ_3, plays the primary role in determining the performance. For a given stage, a given φ_3 at a given Mu_2 yields a certain stage efficiency, a certain work input coefficient, and a certain polytropic head coefficient.

The inlet flow coefficient, i.e., the inlet volume flow, follows suit via the impeller volume ratio.

At the rated point of the multistage compressor, the individual stages operate somewhere in their allowable rating range; some may operate at the optimum, others at the rating range border lines.

The optimum exit flow coefficient can be compromised up to a certain defined limit of efficiency reduction. Stage efficiency and work input factor are then predicted in the same precise manner.

Once measured performance maps have been converted to the described nondimensional curves, based on the similarity parameters φ_3, s, η_p, Mu_2, these maps have become gas independent and may, for design purposes, be applied for any gas, provided Mach numbers are within the range tested.

In other words, the two secondary similarity parameters, work input factor and efficiency, are controlled by the two primary similar parameters, exit flow coefficient and Mach number. The particular combination of tip speed, isentropic exponent, gas constant, and temperature, Mu_2, called Mach number is essential

(see Equations (3), (4), and (8), rather than any single value thereof.

As far as the amount of work input and efficiency are concerned, it does not matter if a stage handling a light gas is operated at high tip speed, or a heavy gas at low tip speed, as long as Mu_2 and φ_3 are equal in both cases. And it also does not affect the performance if a high tip speed stage compresses a hot gas, or a cold gas at low tip speed, as long as Mu_2 and φ_3 stay constant.

So this answers two frequently asked questions:

- Can test results, obtained with a certain gas, be used to accurately predict the performance of the same stage with another gas?
- Can a given compressor stage compress different gases with predictable results?

The answer is yes. The methodology: conduct aerodynamic stage tests over a wide range of Mach numbers; convert test results into dimensionless similarity characteristics; calculate consistent characteristics for the other gas; find performance data from the nondimensional charts; and, stay within the characteristics ranges, established during the measurements.

THE IMPELLER FAMILY

Conjunction of Stage Rating Ranges

The test-deduced rating range, Figure 13, is approximated by an "idealized rating range," Figure 15, limited by two lines of constant φ_3 and by a vertical line of constant φ on the overload side. Note that the lower left hand corner of the rating range, Figure 13, was cut off to avoid low head rises to surge, as they occur for high Mach number applications (see Figure 7). The maximum efficiency dropoff within the idealized rating range is one percent from the optimum. It can be clearly seen—the optimum inlet flow coefficient reduces as the impeller volume ratio goes up (i.e., as Mach number goes down).

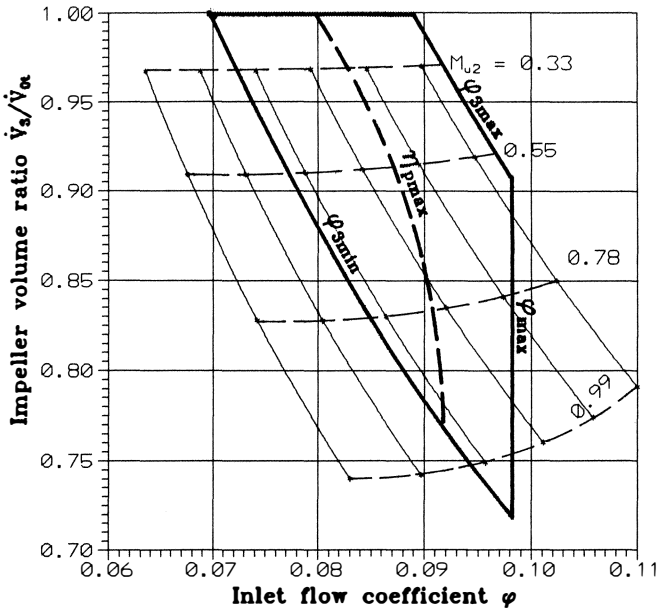

Figure 15. Idealized Stage Rating Range.

The neighboring rating range pertaining to the next higher or lower inlet flow coefficient is added, so that the maximum φ_3-line coincides with the minimum φ_3-line of the next lower stage (Figure 16).

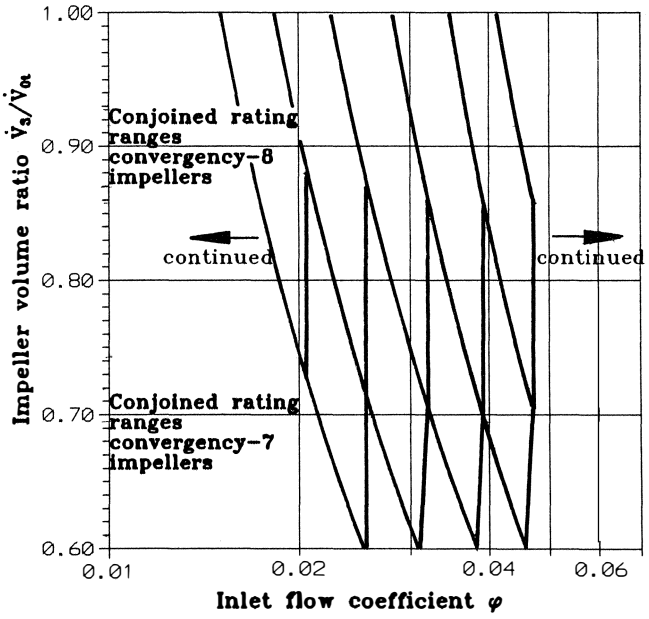

Figure 16. Standard Impeller Selection Diagram (Extract).

In this way, all rating ranges of the so-called "convergency 8" impellers are joined together where "8" is a code for the very strongly rounded-off impeller volume ratio $V_3/V_{ot} \approx 0.8$. Each impeller has a design point where V_3/V_{ot} and φ are fixed, thus determining the impeller geometry. Partload and overload ranges reduce with increasing flow coefficients (i.e., φ_{min}/φ_0 increases and φ_{max}/φ_0 decreases) because high flow coefficient stages are statistically high Mach number stages with shorter performance curves (Figure 7).

Impeller Convergencies

The lower voids are filled in by "convergency 7" impellers, having a volume ratio of roughly 0.7. So rating ranges of these impellers, operating at high Mach numbers (normally handling heavy gases) are limited by two φ_3-lines and two φ-lines to account for shorter performance curves. A convergency 7 impeller of the same inlet flow coefficient has a smaller exit width b_2/d_2 in order to achieve the same exit flow coefficient at a reduced volume ratio (Equation (3)). So the only difference between convergencies 8 and 7 lies in the variation of the convergence of the meridional flow path. The impeller selection diagram (an extract is shown in Figure 16) represents the sum of rating ranges for all members of the impeller family, shown on Figure 1.

It remains to be added that the impeller exit angle increases and the hub/tip ratio decreases with increasing flow coefficient (Figures 17 and 18). The hub/tip ratio curve is dictated by rotordynamics which call for sufficiently high shaft stiffness ratios to avoid close margins between operating and natural frequency and to prevent instability through subsynchronous vibration. Two geometrically different impeller configurations are available—the "O"-line for medium flow coefficient applications, and the "1"-line to allow high flow coefficients in combination with high numbers of stages per casing (Figure 18).

2-D and 3-D impellers

For inlet flow coefficients greater than 0.05, the impeller eye opening increases progressively, bringing about an unacceptably short blade length. So the blade leading edge, in order to assure best efficiencies, must be extended into the eye opening, requiring a blade twist to prevent high incidence losses.

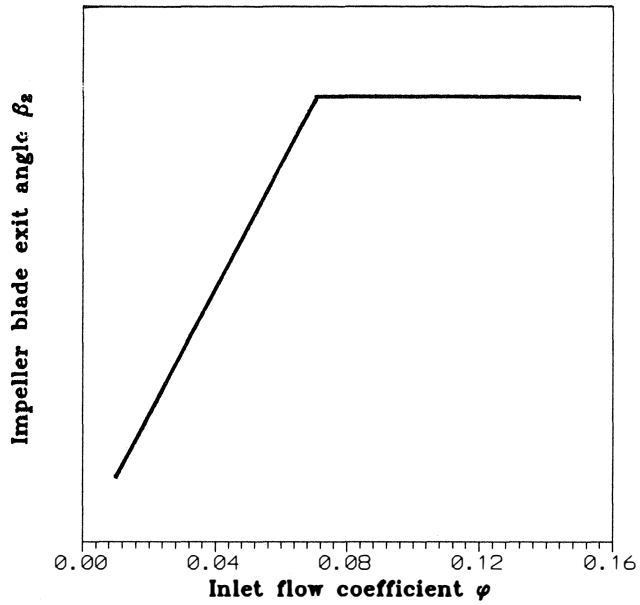

Figure 17. Impeller Blade Exit Angles.

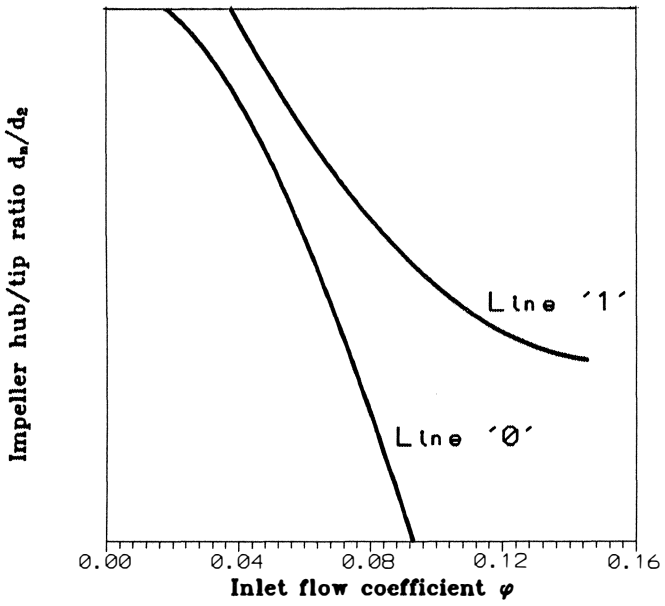

Figure 18. Impeller Hub/Tip Ratios.

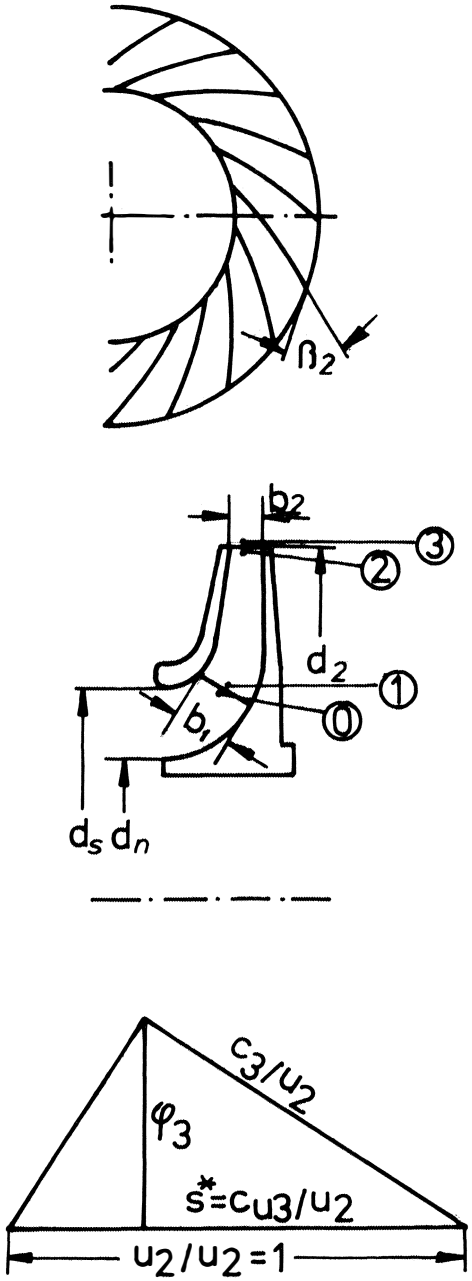

Figure 19. Impeller Schematic and Impeller Exit Velocity Diagram.

These stages with 3-D impellers have at least some three points higher efficiencies than 2-D stages at comparable inlet flow coefficients and considerably better turndowns. Impellers with inlet flow coefficients greater than or equal to 0.05 have 3-D blades.

Blade Cutback and Scaling

The impeller family exclusively consists of these discrete fixed geometry members. Fixed geometry means that the ratios b_1/d_2, b_2/d_2, d_n/d_2, and d_s/d_2 are kept constant for all diameters (Figure 19). No "in between" designs are permitted. The only widely used geometric variation is blade cutback between remaining cover and hub disks, in order to have one more degree of freedom in certain cases. Other variations are very scarce; e.g., eye diameter or exit width modifications.

With the advent of the NC manufacturing era, an unlimited scaling of these impellers within the complete outer diameter range is possible, bringing about an enormous flexibility to adapt to all conditions. By varying the diameter within very small limits for a given impeller type, any stage can be maneuvered into its optimum, rather than letting it operate near its rating range border lines.

Impeller Manufacture

The author's company pioneered two relatively new manufacturing techniques in the field of industrial compressors. In 1974, the first impeller got its cover disk attached by high temperature vacuum brazing with gold/nickel braze, which turned out to be superior to other connecting methods: automated, precisely time/temperature controllable, no obstruction of flow channels by

excessive fillet radii, applicable for extreme narrow widths, and suitable for highest tip speeds.

In 1978, the first 3-D impeller was numerically five-axis-flank-milled from the solid hub forging according to an inhouse developed computer program. This reproducible high quality method made other techniques such as blade die forming with substantially greater manufacturing tolerances obsolete.

For the impeller family described, the five-axis-NC-milling is the sole manufacturing method for all wheel diameters. The limit between cover disk brazing and welding is currently at approximately 800.0 mm diameter with an upward tendency.

FRAME STANDARDIZATION

Whereas different impellers at constant outer diameter are shown in Figure 1, the approximate range chart of the complete modular system is presented in Figure 20, covering actual volume flows from 1,000 to 250,000 m³/h (approx) with 10 frame sizes geometrically stepped at 18 percent diameter increments, representing 40 percent volume flow increments at constant tip speed.

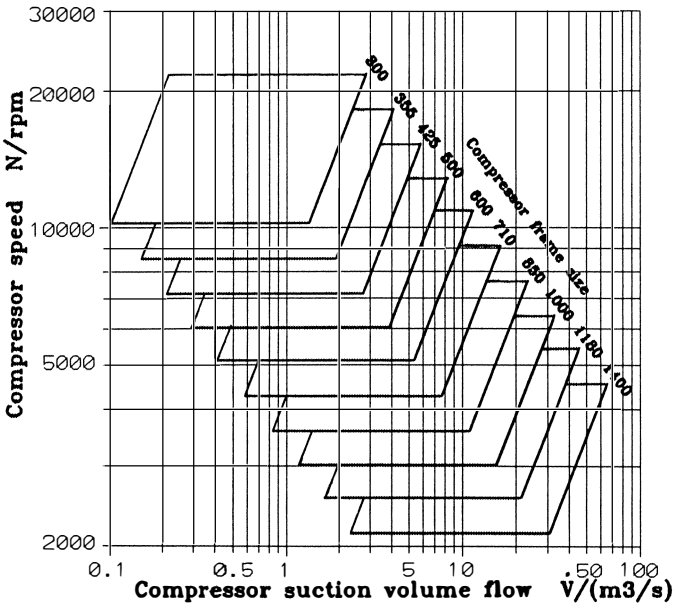

Figure 20. Range Chart for Horizontally and Vertically Split Casings (Approximate).

The frame size designations indicate the maximum possible impeller diameter per casing. Casing head parts are completely standardized for horizontally, and for vertically, split casings, designed to house all commonly specified shaft seals—labyrinth, mechanical contact, floating ring, trapped bushing, and dry gas seals. The casing length varies in the cylindrical middle section and is determined by the number of stages. Casing configurations include inline or back-to-back impeller arrangements. Horizontally split casings used to be cast. However, due to deteriorating quality, a conversion to fabricated casings has been underway for five years (Figure 21).

Barrel casings are normally forged with shear-ring fixed end covers (Figure 22).

DIAPHRAGMS, VOLUTES, NOZZLES

Diaphragms

Per frame size, two diaphragm lines are available: The 1.7- and 1.5-line, representing vaneless diffuser radius ratios of 1.7 and 1.5,

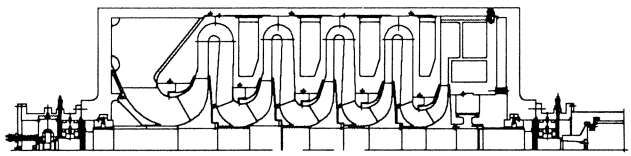

Figure 21. Example: Fabricated Horizontally Split Casing with High Flow Coefficient Impellers, Arranged Inline.

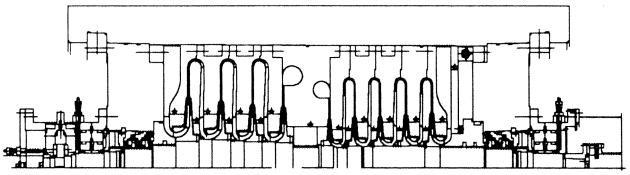

Figure 22. Example: Forged Barrel Type Compressor with Back-to-Back Low Flow Coefficient Impellers.

referenced to a nominal impeller diameter. However, since impeller diameters vary in a given casing, because steps are necessary toward the discharge end depending on Mach number, diffuser radius ratios vary from approximately 1.4 to 1.8. The stage efficiency prediction includes a diffuser/return vane loss model, thus accounting for diffuser radius ratio variations.

Discharge Volutes

Per frame size, ten cast volute sizes (Figure 23) are available for selection, accounting for the enormously varying discharge volume flows of the compressor sections due to variations of impeller diameters, flow coefficients, and impeller tip speeds. A fixed conical diffuser, downstream of the volute, with a standard discharge nozzle diameter, is associated with each standard volute.

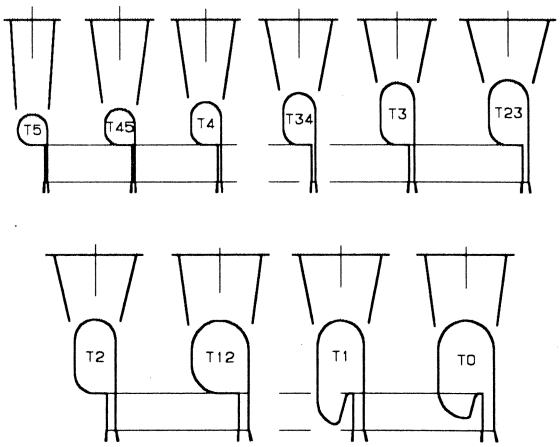

Figure 23. Line of Modular Volutes Per Frame Size.

Suction Nozzles

The fabricated casing design approach allows the use of a range of up to five suction nozzle sizes assigned to each frame size, depending on the impeller type and diameter downstream of the nozzle. The best way to size suction nozzles is by limiting the loss in the inlet duct between the inlet flange and the impeller eye, referenced to the polytropic head of the complete section downstream of the nozzle. This is more appropriate than limiting gas velocities or flange Mach numbers.

SYSTEMATIC PERFORMANCE TESTS ON MODULAR DESIGN STAGES

To confirm the theory and to constitute a reliable data base, numerous aerothermodynamic tests were systematically conducted on the development test stand. Basic air tests were carried out on every other impeller type of the family at a constant diameter of 400.0 mm and with a plenum inlet and a return vane channel outlet.

Variations of these basic tests included:

· long and short vaneless diffusers to find out the efficiency tradeoffs of impellers with the maximum possible diameter in a given casing,

· large and small stage pitches, i.e., the axial distance between two successive stages, to find out the efficiency tradeoff of a compressor casing with the maximum number of stages, as densely squeezed together as possible, and

· cutback of impeller blades between hub and cover disk to find out the effects on efficiency and work input factor.

Detailed test results on these stage geometry variations at low and high Mach numbers and with narrow and wide impellers were published by Lindner [4].

Air tests with convergency 8 impellers were supplemented by tests with the refrigerant R12, with convergency 7 impellers at tip speed Mach numbers of as high as 1.4.

Furthermore, a great number of performance tests have been carried out on contract compressors in the shop test facility during the last 20 years. Thus, characteristic curves could additionally be measured on geometrically similar modular stages with impeller diameters ranging from 300.0 to 1,120.0 mm, making possible a sufficiently accurate determination of the size factor which accounts for the influences of the Reynolds number, relative surface roughness of flow channels, and relative labyrinth clearances. It basically means higher efficiencies for larger machines.

The modular compressor design approach on the basis of detailed systematic aerodynamic stage tests makes theoretical prediction methods obsolete. A great but finite number of modules exist, which have been preengineered, designed, drafted, and aerodynamically tested to a sufficient extent and which have yielded a prediction accuracy that cannot so far be reached by pure theoretical prediction techniques with variable stage geometry concepts, even if the best modelling methods available today are applied.

The strength of the fixed geometry system lies in the fact that only those discrete impellers are being used and their pertaining aerodynamic characteristics that have been measured or have been derived from measurements.

THE APPLICATION OF THE MODULAR DESIGN SYSTEM

How is the system applied for multistage compressors, handling the complete range of industrial gases?

The conventional design of stages is replaced by a selection procedure of stages that have already been designed and whose aerodynamic parameters are known and need not be predicted anymore. After the selection is concluded, the compound performance map of the compressor is calculated by superimposing individual stage performance curves under the specified conditions.

The different steps are as follows:

• The impeller type of the first compressor stage is preselected by the inlet flow coefficient φ with the given inlet volume flow, the tip speed, either determined by the material yield, which in turn is gas dependent, or by the maximum tip speed Mach number, which is relevant for cold heavy gases ($u_2 = Mu_{2max}\, a_0$). A good first choice for the flow coefficient is approximately 0.09 with the aim of not exceeding the maximum impeller diameter of the frame size in question.

The restrictions of rotordynamics dictate that φ can be increased if the number of stages on the shaft is low (say three to four) and that φ must be reduced if the number of stages is high (say seven to 10) and/or if the Mach number is low (e.g., for H_2-rich gases), which leads to successive stages with relatively constant flow coefficients, absorbing a greater axial space than successive stages with diminishing flow coefficients.

• The next step is the calculation of the impeller exit flow coefficient according to Equation (3) with the known b_2/d_2. The impeller volume ratio $\dot{V}_3/\dot{V}_{ot}$ is iteratively calculated from Equations (4), (5), and (6). The resulting φ_3 is used to finally select the impeller. The selection criterion in most cases is to achieve a maximum efficiency. Other criteria may be to attain a large turndown or a specified pressure rise from rated to surge point or to achieve a wide overload. In all of these latter cases, the efficiency must be more or less compromised. The impeller diameter d_2 can be used as an adjusting tool to exactly arrive at the φ_3 wanted—reducing d_2 increasing φ_3 and vice versa, as can be seen from Equations (1) and (3).

To realize a greater than normal operating range which in many cases is more important than a top efficiency, a greater than optimum exit flow coefficient must be the aim.

• Once the suitable impeller type and diameter are selected, the tip speed Mach number Mu_2 is known, the stage efficiency η_p and the work input factor s can be read from the nondimensional φ_3-chart. This serves to determine polytropic head, pressure, and temperature ratio, assuming real gas behavior:

$$h_p = \eta_p\, s\, u_2^2 \tag{14}$$

$$\frac{p_{7t}}{p_{0t}} = \left[\frac{h_p(n_v-1)}{Z_{0t}RT_{0t}n_v}\right]^{\frac{n_v}{n_v-1}} \tag{15}$$

$$\frac{T_{7t}}{T_{0t}} = \left(\frac{p_{7t}}{p_{0t}}\right)^{\frac{n_t-1}{n_T}} \tag{16}$$

p_{7t} = total stage discharge pressure
n_v = polytropic volume exponent
n_T = polytropic temperature exponent
Z_{0t} = suction compressibility factor, total state

Polytropic volume and temperature exponents:

$$\frac{n_v-1}{n_v} = \frac{k_v-1}{k_v} + \frac{1-\eta_p}{\eta_p}\,\frac{k_T-1}{k_T} = f(p,T) \tag{17}$$

$$\frac{n_T-1}{n_T} = \frac{ZR}{c_p}\left(\frac{1}{\eta_p}-1\right)\frac{k_T-1}{k_T} = f(p,T) \tag{18}$$

c_p = isobaric heat capacity

The isentropic volume and temperature exponents:

$$k_v = -\frac{v}{p}\left(\frac{\partial p}{\partial v}\right)_s \tag{19}$$

$$k_T = \frac{1}{1-\frac{p}{T}\left(\frac{\partial T}{\partial p}\right)_s} \tag{20}$$

are calculated from real gas equations LKP (Lee-Kesler-Ploecker), BWRS (Benedict-Webb-Rubin-Starling), RKS (Redlich-Kwong-Soave) and others, (Beinecke and Lüdtke [5]).

v = specific volume

subscripts...entropy = constant

In case of perfect gas behavior (low pressure or high temperature relative to critical state), the exponents reduce to

$$k_v = k_T = \kappa = c_p^0/c_v^0 = f(T) \tag{21}$$

$$\frac{n_v-1}{n_v} = \frac{n_T-1}{n_T} = \frac{\kappa-1}{\kappa\eta_p} = f(T) \tag{22}$$

c_p^0 = perfect gas isobaric heat capacity

c_v^0 = perfect gas isochoric heat capacity

and the compressibility factor becomes

$$Z = 1.0 \tag{23}$$

It should be mentioned that for the polytropic exponents, arithmetic mean values between stage inlet and stage exit are applied.

• With stage discharge pressure and temperature the inlet volume flow of the next stage can be calculated and, at constant rotational speed, inlet and exit flow coefficients, enabling the impeller type selection and so forth. The procedure is repeated for all anticipated stages until the discharge pressure reaches the specified value.

The rotational speed is used as an adjusting tool to exactly reach the desired pressure. If the final speed exceeds allowable values, a further stage must be added.

By varying the actual inlet volume flow, the same method is used to predict the complete performance curve which normally has the form discharge pressure and power input *vs* actual inlet volume flow. Compressor surge is assumed to be reached if either the overall curve reaches its pressure maximum or an individual stage, usually the last, has arrived at its own surge point, which is part of the nondimensional test deduced characteristic. Much in the same way suction throttle, variable speed, or adjustable inlet guide vane maps are calculated.

ASSESSMENT OF THE MODULAR DESIGN SYSTEM

Advantages

The true modular design which uses only fixed relative geometry preengineered and aerodynamically pretested components has many advantages:

· high quality through high performance prediction accuracy in combination with a consistent automated impeller low-tolerance manufacturing process, which eliminates the inadequacies of die forming plus welding,

· speedy quotations and shorter delivery time, since selection of existing components is faster than new design,

· reducing engineering and manufacturing costs without sacrificing quality, thus warranting competitiveness,

· establishing a sound reference basis for modular stages. It is easy to prove the experience of a certain impeller type for wide ranges of outer diameters, tip speeds, polytropic heads, Mach numbers, molecular weights, etc., and

· computer-stored stage geometry and nondimensional performance render it possible to carry out very fast performance predictions of compressors to operate under deviating operating conditions, including different gases.

EXPERIENCES WITH THE MODULAR DESIGN SYSTEM

Coverage

During the past 20 years, some 280 centrifugal compressor casings were sold with some 2,000 impellers altogether (including spare rotors), selected according to the rules of the fixed geometry modular system. Ninety-seven percent of all these applications were covered by the system without any alterations. Three percent had to be geometrically modified. Most of these were the lowest flow coefficient wheels, which had to be reduced in their exit width, because the narrowest available impellers were still too wide for certain applications. In some cases, with very low Mach numbers the exit width had to be increased to account for the high impeller volume ratio (i.e., arriving at a "convergency 9 impeller"). In several applications, the impeller eye diameter had to be increased, and in two cases, the exit angle was reduced to achieve a greater curve slope.

Range of Applications

The number of impellers per shaft ranged from one to nine with five being the statistical majority. Of course, the higher the flow coefficient and the lower the tip speed Mach number, the larger the bearing span and the lower the maximum possible number of wheels on the shaft. These interrelations between aerodynamics and rotordynamics are described in the literature [6].

The impeller experience list comprises:

outer diameters from 280.0 to 1,120.0 mm

polytropic heads per stage: 8.0 to 53.0 kJ/kg

molecular weights: 4.0 to 120.0 kg/ kmol

tip speeds: 150.0 to 330.0 m/s

tip speed Mach numbers: 0.2 to 1.2

As can be seen, stage polytropic heads as high as 53.0 kJ/kg have been realized. This is feasible as long as allowable impeller stresses and allowable tip speed Mach numbers are not exceeded.

Some engineering companies or users specifications call for rigorous polytropic head ceilings per stage of 40.0 or even 30.0 kJ/kg. This is thought to be very conservative and has presumably the background of avoiding mismatch between the stages of a multi-impeller compressor. However, the parameter that governs stage-matching is tip speed Mach number rather than head, as described by the volume ratio across the stage (perfect gas behavior assumed, derivation see APPENDIX):

$$\frac{\dot{V}_{7t}}{\dot{V}_{0t}} = \frac{1}{\left[s(k-1)Mu_2^2+1\right]^{\frac{\kappa\eta_p}{\kappa-1}-1}} \tag{24}$$

$\dot{V}_{7t}$ = stage discharge volume, total state

If the Mach number exceeds certain limits, stage matching is jeopardized. If, for instance, the first stage, operating at a high Mach number, does not produce the predicted stage volume ratio (e.g., due to a smaller efficiency η_p or work input factor s), the second stage receives an increased volume flow which leads to a reduced pressure ratio, because the overload branch of the performance curve is narrow at high Mach numbers and so forth. Thus, a progressive mismatch occurs, resulting in severe negative deviations from the flow, head, and power guarantees.

The cause for the stage mismatch is the combination of high Mach number (i.e., low stage volume ratio) and steep stage performance curve with surge and choke located relatively close to the design point. The mismatch "potential" increases with increasing Mach number and number of stages. So the only way to avoid these difficulties is to limit the Mach number to approximately 1.1 –1.2 for multistage machines, depending on the number of stages.

The polytropic head, on the other hand, does not have to be limited to values below 40.0 or 30.0 KJ/kg as long as Mach numbers are low (e.g., for applications with H_2-rich gas).

Shift of Stage Rating Range

The stage rating range (Figure 15) shows the rating band the compressor stage is allowed to operate in, if the overall compressor is operated at exactly the rated (or guarantee) point. The experience of recent years has shown that a sufficient rise from rated to surge of the polytropic head performance curve is thought to be essential for the proper operation of the discharge pressure controllers and for parallel operation of several compressors. In order to avoid flat curves, it is necessary to prevent part load exit flow coefficients of $\varphi_3/\varphi_{3opt} < 1.0$ and to preferably design compressors, where all stages are rated at the optimum $\varphi_3/\varphi_{3opt} = 1.0$ or with overload ratios of $\varphi_3/\varphi_{3opt} > 1.0$. Depending on the Mach number level, the rated exit flow coefficient ratio can be as high as $\varphi_3/\varphi_{3opt} = 1.1$, or even 1.15. Consequences are an extended operating range and an increased head rise for the price of some minor efficiency reduction and a rotational speed increase. Therefore, during recent years, the allowable stage rating range has shifted from part to overload.

Supplements to the Original Impeller Family

The constant pressure from the market made two supplements within the last five years inevitable:

- A second line of impellers with higher hub/tip ratios had to be introduced:
  - to increase the maximum number of stages per casing (i.e., to avoid multicasing solutions to a certain extent)
  - to use high flow coefficient impellers for multistage compressors (i.e., to increase the efficiency)

The original hub/tip ratio line "0" and the supplemental high hub/tip ratio line "1" are shown in Figure 18.

- The impeller family had to be supplemented by three high flow coefficient impeller types:
  - to bring about a frame size decrease for a number of applications without sacrificing efficiency
  - to increase efficiencies by avoiding very low flow coefficients at the discharge end of the compressor

The high flow coefficient supplements are shown on Figure 1, top right and side, convergency 8 line.

Fulfillment of Guarantees

As far as the usual head, flow, power, and surge guarantees are concerned,the modular design system was extremely successful. The percentage of compressors which had to be redesigned due to missed performance, was well below one percent. Only a handful of impellers had to be blade trimmed to adjust pressure ratios. The vast majority attained the power guarantee without making use of the API 617 tolerance of plus four percent granted to manufacturers. No penalties had to be paid, and no compressor was rejected due to excessive power consumption.

SUMMARY AND CONCLUSION

The modular design system is based on scalable fixed geometry components, which operate under limited deviations from the principles of aerodynamic similarity. The philosophy is demonstrated by consistently evaluating an example of a measured compressor stage, beginning with the conventional performance map, via gas-independent nondimensional characteristics and ending with the stage rating range, which replaces the conventional design point of adaptable-geometry components.

The aero-system comprises the family with 2-D and 3-D bladed impellers, standard lines of diaphragms, volutes, and nozzles assigned to ten horizontally and eight vertically split frame sizes.

Systematically conducted modular stage performance tests, in combination with the high quality 5-axis NC-milling of impellers, yield an unprecedented performance prediction accuracy.

The practical application of the modular system describes how an arbitrary compressor is designed and its performance map determined.

The fact that 97 percent of all applications were covered by the system without any modifications, and that the guarantee fulfillment rate was higher than 99 percent, demonstrates the success of the described design system.

So it is thought that the 20 years of experience with the consistently utilized modular system is a long enough time period to have sufficiently demonstrated the feasibility, usefulness, versatility, reliability, and precision of this design approach for chemical, petrochemical, refrigeration, refinery, and natural gas field applications.

APPENDIX

Derivation of Equation (4)

Impeller volume ratio, inlet total to exit static:

Assumptions: perfect gas, impeller disk windage and shroud leakage loss neglected.

$$\frac{\dot{V}_3}{\dot{V}_{0t}} = \frac{T_{3s}}{T_{0t}} \frac{1}{\Pi_{Ls}} = \frac{\Pi^e_{Ls}}{\Pi_{Ls}} = \frac{1}{\Pi_{Ls}^{1-e}} \qquad \text{(A-1)}$$

T_{3s} = absolute static temperature impeller exit

T_{0t} = absolute total temperature impeller inlet

$\Pi_{Ls} = \frac{p_{3s}}{p_{0t}}$ impeller pressure ratio, inlet total to exit static

$$e = \frac{\kappa - 1}{\kappa \eta_{pLs}} \qquad \text{(A-2)}$$

η_{pLs} = polytropic impeller efficiency, inlet total to exit static

$\kappa = c_p^0/c_v^0$ = ratio of heat capacities, perfect gas

Enthalpy difference, total-to-total (Euler head):

$$\Delta h = \Delta h_{Ls} + \frac{c_3^2}{2} = su_2^2 \qquad \text{(A-3)}$$

Δh_{Ls} = impeller enthalpy difference, inlet total to exit static

c_3 = absolute velocity impeller exit
s = work input coefficient
u_2 = impeller tip speed

Reaction:

$$r = \frac{\Delta h - \frac{c_3^2}{2}}{\Delta h} = 1 - \frac{c_3^2}{2\Delta h} = 1 - \frac{c_3^2}{2su_2^2} = 1 - \frac{\varphi_3^2 + s^2}{2s} \qquad \text{(A-4)}$$

$\varphi_3 = \frac{c_{m3}}{u_2}$ impeller exit flow coefficient

c_{m3} = meridional velocity, impeller exit

From velocity diagram, Figure 19 (windage and shroud leakage neglected):

$$\left(\frac{c_3}{u_2}\right) = \varphi_3^2 + s^2 \qquad \text{(A-5)}$$

Impeller enthalpy difference, with Equation (A-3):

$$\Delta h_{Ls} = RT_{0t} \frac{\kappa}{\kappa - 1} \left(\Pi_{Ls}^{e} - 1\right) = \Delta h - \frac{c_3^2}{2} \qquad \text{(A-6)}$$

R = gas constant

Equations A-4 and A-6 combined:

$$RT_{0t} \frac{\kappa}{\kappa - 1} \left(\Pi_{Ls}^{e} - 1\right) = \Delta hr = su_2^2 r \qquad \text{(A-7)}$$

Impeller pressure ratio, perfect gas:

$$\Pi_{Ls} = \left[1 + s(\kappa - 1)r \frac{u_2^2}{\kappa RT_{0t}}\right]^{\frac{1}{e}} \qquad \text{(A-8)}$$

$$\Pi_{Ls} = \left[1 + s(\kappa - 1)r\,Mu_2^2\right]^{\frac{1}{e}} \qquad \text{(A-9)}$$

Combining Equations (A-1) with Equation (A-9):

$$\frac{\dot{V}_3}{\dot{V}_{0t}} = \frac{1}{\left[1 + s(\kappa - 1)r\,Mu_2^2\right]^{\frac{1}{e} - 1}} \qquad \text{(A-10)}$$

Replacing total-to-static by total-to-total polytropic impeller efficiency:

Definition total-to-static polytropic impeller efficiency:

$$\eta_{pLs} = \frac{h_{pLs}}{\Delta h_{Ls}} = \frac{h_{pLs}}{\Delta h - \frac{c_3^2}{2}} \qquad \text{(A-11)}$$

h_{pLs} = polytropic impeller head, inlet total to exit static

Definition total-to-total polytropic impeller efficiency:

$$\eta_{pL} = \frac{h_{pL}}{\Delta h} = \frac{h_{pLs} + \frac{c_3^2}{2}}{\Delta h} \qquad \text{(A-12)}$$

h_{pL} = polytropic impeller head, total-to-total

From Equation (A-11) attain

$h_{pLs} = h_{pL} - \frac{c_3^2}{2}$ and $h_{pL} = \Delta h \eta_{pL}$:

$$\eta_{pLs} = \frac{\Delta h \eta_{pL} - \frac{c_3^2}{2}}{\Delta h - \frac{c_3^2}{2}} = \frac{\eta_{pL} - \frac{c_3^2}{2\Delta h}}{1 - \frac{c_3^2}{2\Delta h}} \qquad \text{(A-13)}$$

and with Equation (A-4)

$$\eta_{pLs} = \frac{\eta_{pL} + r - 1}{r} \qquad \text{(A-14)}$$

Using Equation (A-14)

$$x = \frac{1}{e} - 1 = \frac{\kappa \eta_{pLs}}{\kappa - 1} - 1 = \frac{\kappa}{\kappa - 1}\left(\frac{\eta_{pL} + r - 1}{r}\right) - 1$$

$$x = \frac{r + \kappa(\eta_{pL} - 1)}{r(\kappa - 1)} \qquad \text{(A-15)}$$

Final formula for the impeller volume ratio:

$$\frac{\dot{V}_3}{\dot{V}_{0t}} = \frac{1}{[1 + s(k-1)\,r\,Mu_2^2]^x} \quad ; \quad x = \frac{r + \kappa(\eta_{pL} - 1)}{r(\kappa - 1)} \qquad \text{(A-16)}$$

Derivation of Equation (24):

Stage volume ratio, total-to-total; perfect gas assumed:

$$\frac{\dot{V}_{7t}}{\dot{V}_{0t}} = \frac{T_{7t}}{T_{0t}} \frac{1}{\Pi_t} = \frac{\Pi_t^c}{\Pi_t} = \frac{1}{\Pi_t^{1-c}} \qquad \text{(A-17)}$$

T_{7t} = absolute total stage discharge temperature
Π_t = stage pressure ratio, total-to-total

$$c = \frac{\kappa - 1}{\kappa \eta_p}$$

η_p = polytropic stage efficiency, total-to-total

Enthalpy difference, total-to-total (Euler head):

$$\Delta h = RT_{0t} \frac{\kappa}{\kappa - 1} (\Pi_t - 1)^c = su_2^2 \quad \text{(A-18)}$$

$$\Pi_t = \left[1 + s(\kappa - 1) r \frac{u_2^2}{\kappa R T_{0t}}\right]^{\frac{1}{c}} = \left[1 + s(\kappa - 1) r Mu_2^2\right]^{\frac{1}{c}} \quad \text{(A-19)}$$

Final formula for the stage volume ratio:

$$\frac{\dot{V}_{7t}}{\dot{V}_{0t}} = \frac{1}{\left[1 + s(\kappa - 1) Mu_2^2\right] \frac{\kappa \eta_p}{\kappa - 1} - 1} \quad \text{(A-20)}$$

Slip/Work Input Factor Ratio

Gas power from Euler head, shroud leakage and disk friction:

$$\dot{m} s u_2^2 = (\dot{m} + \Delta\dot{m}) u_2 c_{u3} + M_F \omega \quad \text{(A-21)}$$

$$LF = 1 + \frac{\Delta\dot{m}}{\dot{m}} \quad \text{shroud leakage factor} \quad \text{(A-22)}$$

$$M_F = C_M \frac{\rho_3}{2} \omega^2 r_2^5 \quad \text{frictional torque of 2-sided disk} \quad \text{(A-23)}$$

$$\omega = \frac{u_2}{r_2} \quad \text{angular velocity} \quad \text{(A-24)}$$

$$P_F = M_F \omega = C_M \frac{\rho_3}{2} u_2^3 r_2^2 \quad \text{frictional power} \quad \text{(A-25)}$$

Impeller slip:

$$s^* = \frac{c_{u3}}{u_2} = \frac{\dot{m} s u_2^2 - C_M \frac{\rho_3}{2} u_2^3 r_2^2}{LF \dot{m} u_2^2} \quad \text{(A-26)}$$

$$LF\dot{m} = \rho_3 c_{m3} \pi 2 r_2 b_2 \quad \text{impeller mass flow} \quad \text{(A-27)}$$

$$C_M = \frac{0.102 (s/r_2)^{0.1}}{Re^{0.2}} \quad \text{torque coefficient acc. to Daily and Nece [7]} \quad \text{(A-28)}$$

$$Re = \frac{u_2 r_2}{\nu_3} \quad \text{Reynolds number} \quad \text{(A-29)}$$

$$s^* = \frac{s}{LF} - \frac{C_M}{8\pi\varphi_3 \frac{b_2}{d_2}} \quad \text{(A-30)}$$

Slip/work input factor ratio:

$$\frac{s^*}{s} = \frac{1}{LF} - \frac{C_M}{8\pi s \varphi_3 \frac{b_2}{d_2}} \quad \text{(A-31)}$$

ρ_3 = density in chamber
$\dot{m}$ = compressor mass flow, incl. balance piston leakage
r_2 = impeller outer radius
ν_3 = kinematic viscosity in chamber
s = work input factor

C_M is in the range of 0.003 to 0.006 for most applications

REFERENCES

1. Sheets, H.E., "Nondimensional Compressor Performance for a Range of Mach Numbers and Molecular Weights," ASME-Paper No. 51-SA-19 (1951).
2. Strub, R.A., et al., "Influence of the Reynolds Number on the Performance of Centrifugal Compressors," ASME-Paper No. 87-GT-10 (1987).
3. Lüdtke, K., "Industrial Centrifugal Compressors: The Influence of the Impeller Diffusion on the Stage Performance," ASME-Paper No. 89-GT-233 (1989).
4. Lindner, P., "Aerodynamic Tests on Centrifugal Process Compressors—Influence of Diffuser Diameter Ratio, Axial Stage Pitch and Impeller Cutback," Transactions of the ASME, Journal of Engineering for Power (October 1983).
5. Beinecke, D. and Lüdtke, K., "Die Auslegung von Turboverdichtern unter Beruecksichtigung des realen Gasverhaltens," VDI-Berichte No. 487 (1983).
6. Lüdtke, K., "Turboverdichter," Dubbel Taschenbuch fuer den Maschinenbau, 17th Edition, pp. R65-75 (1990).
7. Daily, J. W. and Nece, R. E., "Chamber Dimension Effects on Induced Flow and Frictional Resistance of Enclosed Rotating Disks" ASME-Paper No. 59-Hyd-9 (1959).